ELSEVIER

International Journal of Mass Spectrometry 185/186/187 (1999) 989–1001

International Journal of Mass Spectrometry

Activation of methane by Ti^+: a cluster assisted mechanism for σ-bond activation, experiment, and theory

Petra A.M. van Koppen[a,*], Jason K. Perry[b], Paul R. Kemper[a], John E. Bushnell[a], Michael T. Bowers[a,b,*]

[a]*Department of Chemistry, University of California, Santa Barbara, CA 93106, USA*
[b]*First Principles Research, Inc., 8391 Beverly Blvd. Suite 171, Los Angeles, CA 90048, USA*

Received 21 September 1998; accepted 12 November 1998

Abstract

Reactions of Ti^+ with methane were studied by both temperature-dependent equilibrium measurements and density functional theory. Experimentally, we observed $Ti(CH_4)_n^+$ clusters ($n = 1$–5) and the H_2 elimination products $(CH_4)Ti(CH_3)_2^+$, $Ti(CH_3)_2^+$, and $(CH_4)_2Ti(C_2H_4)^+$. The binding energies for the $Ti(CH_4)_n^+$ clusters were measured to be 16.8 ± 0.6, 17.4 ± 0.6, 6.6 ± 1.5, 9.8 ± 0.8, 5.1 ± 0.7 kcal/mol for $n = 1$–5, respectively. From analysis of the association entropies it was clear that the first solvation shell was completed at $n = 4$ and the fifth CH_4 ligand began the second shell. For the addition of the third methane ligand to Ti^+, we observed σ-bond activation to be competitive with adduct formation and dehydrogenation of the cluster produced $(CH_4)Ti(CH_3)_2^+$. Theoretically we characterized the $Ti(CH_4)_n^+$ clusters ($n = 1$–3) and reproduced the trend in binding energies observed experimentally. We also calculated many local minima and several transition states on the potential energy surfaces for dehydrogenation for $n = 1$–3. In agreement with experiment, we found dehydrogenation of the first methane to be highly unfavorable, dehydrogenation of the second to be slightly unfavorable, and dehydrogenation of the third to be slightly favorable under the given conditions. Moreover, addition of a fourth methane resulted in further dehydrogenation and formation of an ethylene ligand bound to the metal center, $(CH_4)_2Ti(C_2H_4)^+$. Hence, it appears that methane can be converted to ethylene in a cluster mediated σ-bond activation mechanism using first row transition metal centers at thermal energies. (Int J Mass Spectrom 185/186/187 (1999) 989–1001) © 1999 Elsevier Science B.V.

Keywords: Methane activation; cluster assisted sigma bond activation; Transition metal; Titanium; Density functional theory

1. Introduction

Gas-phase σ-bond activation of methane has not been previously observed to be spontaneous for first row transition metal ions. Experimentally, under single collision conditions, all $M^+ + CH_4$ reaction channels have been determined to be endothermic for first row transition metal ions [1], a result consistent with theory [2,3]. Reactivity has been found to increase as the size of the alkane increases, with many first row metals capable of dehydrogenating and demethanating propane [4]. Under multiple collision

* Corresponding authors. E-mail: petra@chem.ucsb.edu

Dedicated to Professor Michael T. Bowers on the occasion of his 60th birthday.

PII S1387-3806(98)14269-0

conditions, first row transition metal ions, Co^+ and Fe^+, were observed to react with methane to produce $M(CH_4)_n^+$ clusters, $n = 1$–4, but neither Co^+ or Fe^+ activates methane; no elimination channels were observed [5–7]. Of second row transition metal ions only Zr^+ has been reported to dehydrogenate CH_4 spontaneously [8,9]. For many third row transition metal ions, however, multiple dehydrogenation reactions were observed, leading to the oligomerization of methane [10,11].

Recently a new mechanism, cluster assisted σ-bond activation, was proposed to explain the chemistry of Sc^+ reacting with dihydrogen [12]. A detailed analysis of the apparently "simple" equilibrium between Sc^+ and H_2 indicated that both the adduct, $Sc(H_2)^+$, and the inserted species, H–Sc^+–H, were present. A kinetic analysis indicated H_2 activation occurred only after the addition of the third H_2 ligand. Even though the activation of H_2 by ground state Sc^+ to form the inserted species, H–Sc^+–H, is exothermic, theory predicts [13] an insertion barrier of approximately 19.0 kcal/mol. The addition of the third H_2 ligand appears to provide sufficient stabilization energy to bring the insertion barrier below the energy of the reactants, ground state ^3D $(4s3d)$ $Sc^+ + H_2$.

The possibility of a cluster assisted σ-bond activation mechanism inspired us to further explore reactions of first row transition metal ions with methane. Experimentally, the activation of methane by ground state Ti^+ to form the inserted species, H–Ti^+–CH_3, is estimated [14] to be exothermic by 12 kcal/mol [15,16] but dehydrogenation at thermal energies is endothermic by 18.9 kcal/mol [15]. A theoretical study by Hendrickx et al. [3] predicts the H–Ti^+–CH_3 species to be endothermic by 1.1 kcal/mol and the transition state to insertion to be located 15.3 kcal/mol above the ground state asymptote, ^4F $(4s3d^2)$ $Ti^+ + CH_4$. In the high-pressure environment of the flow tube Tonkyn et al. [4] found that at 300 K, Ti^+ ligates five methane ligands but does not activate methane; no elimination products were observed. A question of particular interest is whether or not a cluster assisted σ-bond activation mechanism is possible for Ti^+ reacting with $n CH_4$, and if so under what conditions.

To address this question, reactions of Ti^+ with methane were studied by both temperature-dependent equilibrium measurements and density functional theory (DFT). Experimentally, we accurately measured the binding enthalpies and entropies for the sequential addition of five CH_4 ligands and reproduced the trend for the first three ligands with theory. For the addition of the third methane to Ti^+, we observed a slow approach to equilibrium and measured the rate to attain equilibrium as a function of temperature. The observed H_2 elimination channels are discussed and a cluster assisted σ-bond activation mechanism is proposed that is consistent with theory.

2. Experiment

Details of the experimental apparatus [17] have been published, and sources of error have also been discussed extensively [12]. In the experiments reported here, titanium ions were formed by surface ionization of $TiCl_4$ and their electronic state distribution was determined by ion chromatography [18]. The ions were accelerated to 5 keV, mass selected with a double focusing, reverse geometry mass spectrometer, decelerated to approximately 3–5 eV, and injected into a reaction cell containing $\sim 7 \times 10^{16}$ molecules/cm^3 of methane (2.2 Torr at 300 K). The ions were quickly translationally and electronically [18,19] thermalized via collisions with CH_4, and were moved through the cell under the influence of a small electric field ($E/N < 3 \times 10^{-17}$ V cm^2). The CH_4 pressure in the reaction cell is monitored directly with a capacitance manometer and the pressure was varied to ensure equilibrium was attained. Cell temperatures were varied using a flow of heated or cooled N_2, and temperatures measured using a thin-film platinum resistor. Ions exiting the cell were quadrupole mass analyzed and counted.

In the equilibrium experiment [20], product/parent ion ratios were measured as a function of reaction time, $(E/N)^{-1}$. This time was varied by changing the drift voltage across the cell. As the drift time was increased the product/parent ion ratios eventually become constant, indicating equilibrium had been

reached. The ratios were converted to equilibrium constants and standard free energies [20]. A plot of ΔG° versus T yielded straight lines for all systems with an intercept equal to ΔH_T° and a slope equal to ΔS_T°. Standard statistical thermodynamic methods were used to obtain ΔH_0° from ΔH_T° and ΔS_T°. This plot is functionally equivalent to a van't Hoff plot, but it is more convenient for our data analysis.

Rate coefficients were also determined for the third clustering reaction. At very short reaction times the equilibrium involves simple methane addition (reaction 1).

$$Ti(CH_4)_2^+ + CH_4 \rightleftharpoons Ti(CH_4)_3^+ \quad (1)$$

As reaction time increases, C–H bond activation competes with adduct formation. As will be discussed, experimental results show that methane is more strongly bound in the inserted species, $(H)(CH_3)Ti(CH_4)_2^+$, than in the adduct, $Ti(CH_4)_3^+$. Thus, the slope of the equilibrium constant as a function of time, reflects the increasing fraction of the formation of the inserted species, $(H)(CH_3)Ti(CH_4)_2^+$. To obtain the rate constant for C–H bond activation, we used a standard $\ln(I/I_0)$ versus time analysis. Specifically, we measured the $n = 3$ to $n = 2$ ratio (corresponding to the addition of the third and second methane, respectively) as a function of time at different temperatures, ranging from 300 to 550 K. In addition, we measured the pressure of the methane and the mobilities as a function of temperature to determine the reaction time as a function of temperature. Together these yield the insertion rate coefficient in units of cm^3/s. Plotting the logarithm of the rate constant as a function of inverse temperature yields the activation energy as the slope. Note that the inserted species does cluster further but this does not affect the rate measurement because subsequent methane clusters are in equilibrium (the equilibrium concentration of the $(H)(CH_3)Ti(CH_4)_2^+$ species may be off by a constant factor but the slope of the $\ln\{[Ti(CH_4)_3^+ + (H)(CH_3)Ti(CH_4)_2^+]/[Ti(CH_4)_2^+]\}$ versus time plot is independent of this constant offset.

3. Computational details

We have performed density functional calculations to help characterize the reactions of Ti^+ with up to three methanes. All calculations were done using the Becke-3-LYP functional [21]. Geometry optimizations were first performed using Hay and Wadt's Ne core ECP in conjunction with their standard valence double-ζ basis set [22] for Ti and a 6-31G** basis set [23] for C and H. Final single point energies were evaluated using a valence triple-ζ contraction of the Hay and Wadt basis set for Ti and a 6-311 + G** basis set [24] for C and H. The triple-ζ contraction of the Ti basis set proved to be significantly better than the double-ζ contraction in regard to the calculation of Ti^+ state splittings. In particular, the ground state of Ti^+ is known to be ^4F (s^1d^2) with a low-lying $^4F(d^3)$ state just 2.46 kcal/mol higher in energy. With the standard double-ζ contraction, the states are reversed with a splitting of -17.62 kcal/mol. With the triple-ζ contraction, the states are still reversed, but by only -0.53 kcal/mol (a total error in the state splittings of only 2.99 kcal/mol).

Only the lowest energy state and the geometry of each intermediate species are reported, although in most instances a number of other low-lying states or conformations were found. Zero point energies, temperature corrections, and entropies were calculated for all species at the same level used to find the geometries. Frequencies were unscaled in the calculation of these quantities. Transition states were optimized using a linear/quadratic synchronous transit (LST/QST) procedure. All calculations were done using the Jaguar program from Schrödinger Inc. [25].

4. Results and discussion

4.1. $Ti(CH_4)_n^+$ association clusters

The observed free energy, ΔG, as a function of temperature for the equilibria (reaction 2) are shown in Fig. 1.

$$Ti(CH_4)_{n-1}^+ + CH_4 \rightleftharpoons Ti(CH_4)_n^+ \ (n = 1\text{–}5) \quad (2)$$

The association enthalpies, ΔH_T°, and entropies, ΔS_T°, given by the intercepts and slopes, respectively, are

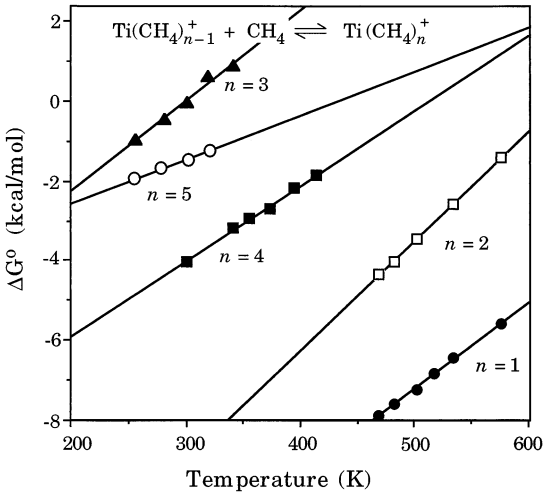

Fig. 1. The plots of ΔG° vs. temperature for the sequential addition of CH_4 molecules to ground state Ti^+ ions. The values of ΔG° are deduced from measured equilibrium constants as described in the text.

listed in Table 1. The values of ΔH_0°, obtained from ΔH_T° and ΔS_T° using standard statistical thermodynamic methods, and the theoretical data on the sequential methane binding energies are reported in Table 2.

A linear fit to the ΔG_T° versus temperature data (Fig. 1) for the first Ti^+–CH_4 association gives ΔH_T° and ΔS_T° values of -17.9 ± 0.6 kcal/mol and -21.5 ± 1.1 cal/mol K, respectively (Table 1). The resulting bond dissociation energy (BDE) from the statistical mechanical fit to the data [20] is 16.8 ± 0.6 kcal/mol (Table 2). From our DFT calculations, the ground state of $Ti(CH_4)^+$ has the methane coordinated to the Ti^+ through three C–H bonds, in an η^3 configuration, (shown in Fig. 2), but a slight Jahn–Teller distortion reduces the symmetry from C_{3v} to C_s. The spin of the complex is quartet, but the Ti^+ configuration changes from s^1d^2 to dominantly d^3 character. The enthalpy of complexation was calculated to be $\Delta H_0^\circ = -15.7$ kcal/mol (or $D_0 = 15.7$ kcal/mol, Table 2) with respect to the calculated asymptote of the ground state, ^4F (s^1d^2) $Ti^+ + CH_4$, in good agreement with the experimental value of 16.8 ± 0.6 kcal/mol.

Table 1
Experimental ΔH_T° and ΔS_T° for $Ti(CH_4)_{n-1}^+ + CH_4 \rightarrow Ti(CH_4)_n^+$

n	$-\Delta H_T^\circ$ [a]	$-\Delta S_T^\circ$ [b]	Temperature range[c]
1	17.9 ± 0.6	21.5 ± 1.1	470–580
2	17.2 ± 0.4	27.5 ± 0.8	470–580
3	6.8 ± 1.3	22.7 ± 4.2	255–340
4	9.6 ± 0.6	18.9 ± 1.7	300–415
5	4.7 ± 0.5	11.0 ± 2.0	255–320

[a] In units of kcal mol^{-1}.
[b] In units of cal mol^{-1} K^{-1}.
[c] In units of K.

Table 2
Derived experimental (ΔH_0°) and theoretical binding energies (D_e and D_0) for $Ti(CH_4)_{n-1}^+ + CH_4 \rightarrow Ti(CH_4)_n^+$

n	Experiment[a,b] $-\Delta H_0^\circ$	Theory[a] D_e	Theory[a] D_0
1	16.8 ± 0.6	16.1	15.7
2	17.4 ± 0.6	16.2	14.9
3	6.6 ± 1.5	3.4	2.3
4	9.8 ± 0.8	...	...
5	5.1 ± 0.7	...	...

[a] In units of kcal mol^{-1}.
[b] The uncertainties reflect the uncertainties in ΔH_T° in addition to the uncertainties due to the statistical mechanical modeling.

The bonding in $Ti(CH_4)^+$ is similar to that reported by Perry, Ohanessian, and Goddard [26] for the η^3 coordination of $Co(CH_4)^+$. For Co^+, a d^8 metal ion, the d_σ orbital, which points directly at the ligand, is doubly occupied. This orbital hybridizes with the empty 4*s* orbital to reduce its density in the *z* direction and increase it in the *x* and *y* directions, thus reducing

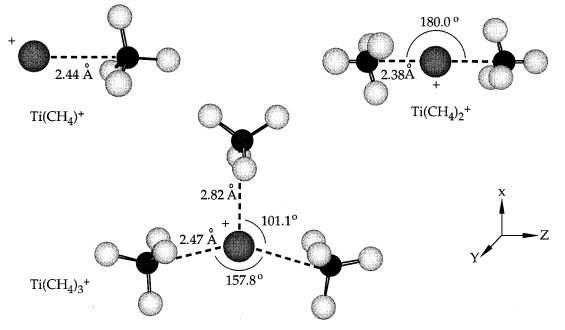

Fig. 2. Geometries of the $Ti(CH_4)_n^+$ complexes calculated: $n = 1$ with C_s symmetry; $n = 2$ with C_{2h} symmetry; $n = 3$ with C_{2v} symmetry.

its repulsion to the ligand. The remaining *d* orbitals form linear combinations such that the two orbitals that are singly occupied have lobes that point toward the methane C–H bonds while the two remaining orbitals that are doubly occupied have lobes that point to the space between the C–H bonds. This unique configuration of the metal electrons allows for a minimization of both metal *d*–*d* repulsion and metal–ligand repulsion. In the case of $Ti(CH_4)^+$, the d^3 metal has the d_σ orbital singly occupied. This orbital hybridizes with the empty 4*s* orbital to reduce repulsion to the ligand. The remaining *d* orbitals form linear combinations such that the two singly occupied orbitals have lobes that point towards the space between the C–H bonds and the two remaining empty orbitals have lobes that point directly at the C–H bonds. Based on the results for $Co(CH_4)_n^+$, a second methane may be expected to bond similarly to Ti^+, but bonding of a third and fourth methane may require significant changes to the electronic structure [6].

The experimental data for the second association (Fig. 1) yield ΔH_T° and ΔS_T° values of -17.2 ± 0.4 kcal/mol and -27.5 ± 0.8 cal/mol K, respectively (Table 1). The resulting BDE, 17.4 ± 0.6 kcal/mol (Table 2), is slightly greater than the first methane (16.8 ± 0.6 kcal/mol). The DFT results indicate that the first and second methane coordinate to the metal in a similar fashion with staggered methanes and a CH_4–Ti–CH_4 angle of 180° (Fig. 2). Again the geometry is slightly Jahn–Teller distorted from D_{3d} symmetry to C_{2h} symmetry. The enthalpy of complexation for the second methane was calculated to be $\Delta H_0^\circ = -14.9$ kcal/mol ($D_0 = 14.9$ kcal/mol, Table 2), a slight decrease as compared to the first methane. Even though experimentally we find a slight increase in the BDE for the second methane as compared to the first methane, both theory and experiment predict similarly strong BDEs for both the first and second methanes.

The experimental data for the third association (Fig. 1) yield ΔH_T° and ΔS_T° values of -6.8 ± 1.3 kcal/mol and -22.7 ± 4.2 cal/mol K, respectively (Table 1). The resulting BDE, 6.6 ± 1.5 kcal/mol (Table 2), is much smaller than the BDEs of either the first or second methane (16.8 ± 0.6 and 17.4 ± 0.6 kcal/mol, respectively). Theory shows that the third methane is significantly farther from the metal center than the first two (Fig. 2), which is reflected in the low BDE calculated, $D_0 = 2.3$ kcal/mol (Table 2). As with $Co(CH_4)_3^+$, the ideal bonding situation which exists for the first two methanes is necessarily compromised in order to bond a third methane. In particular, the *s*–*d* hybridization reduces metal–ligand repulsion along the *z* axis but it *increases* metal ligand repulsion in the *xy* plane. Therefore at most only two ligands can take advantage of it. For the first two methane bonds to remain strong by maintaining *s*–*d* hybridization, the third methane must be weaker and further from the metal center. Alternatively, the reduction or elimination of *s*–*d* hybridization could lead to three equivalent methane bonds, in which the first two are weakened in order to strengthen the third. Theory indicates that the former is slightly more favorable for $Ti(CH_4)_3^+$, with a ground state geometry having C_{2v} symmetry. Overall, the calculations underestimate the binding energies of the first three methanes to Ti^+ by 2–4 kcal/mol but reproduce the trend well (Table 2).

The experimental data for the fourth cluster (Fig. 1) yield ΔH_T° and ΔS_T° values of -9.6 ± 0.6 kcal/mol and -18.9 ± 1.7 cal/mol K, respectively (Table 1). The resulting BDE, 9.8 ± 0.6 kcal/mol (Table 2), is significantly larger than the third methane (6.6 ± 1.5 kcal/mol) but smaller than the BDE of either the first or second methane (16.8 ± 0.6 and 17.4 ± 0.6 kcal/mol, respectively). The trend in binding energies for $Ti(CH_4)_n^+$, $n = 1$–4, follows that for $Co(CH_4)_n^+$ very closely (first $\approx$ second $\gg$ third $<$ fourth). In both cases this trend appears to be dominated by the issue of *s*–*d* hybridization, as explained. The fourth methane is found to be more strongly bound than the third because the energy associated with a loss of *s*–*d* hybridization, or weakening of the first two bonds, is shared between the third and fourth methane ligands instead of just the third methane. Overall, methane is systematically more strongly bound to Co^+ than to Ti^+. This occurs primarily because the Co^+ ion is more compact resulting in shorter M^+–methane bonds and hence stronger bonds.

For the association of the fifth methane, the values

of ΔH_T° and ΔS_T° are -4.7 ± 0.5 kcal/mol and -11.0 ± 2.0 cal/mol K, respectively (Table 1) and the BDE is 5.1 ± 0.7 kcal/mol (Table 2). A linear fit to the ΔG_T° versus temperature data (Fig. 1) for the fifth methane clearly shows a significant decrease in slope and a correspondingly small change in entropy (-11.0 ± 2.0 cal/mol K) relative to the first four methanes (ranging from -18.9 to -27.5 cal/mol K). The decrease in BDE and the large increase in ΔS are consistent with the fifth CH_4 ligand going into the second solvation shell. Hence, the first solvation shell fills with the addition of the fourth CH_4 ligand.

We have observed similar decreases in the bond dissociation energies and increases in association entropy in $M(H_2)_n^+$ systems [27–29]. For example, for M = Co, Ni, and Cu the first solvation shell appears to be completed with six, five, and four H_2 molecules, respectively [27–29]. The association entropy for H_2 ligands in the first solvation shell ranged from -18.1 to -25.1 cal/mol K. However, for the addition of H_2 to $Co(H_2)_6^+$, $Ni(H_2)_5^+$, and $Cu(H_2)_4^+$, the values for ΔS_T° are significantly larger, -8.3, -10.5, and -12.0 cal/mol K, respectively [27–29], indicating substantially increased motion for this final H_2 ligand about the metal center.

4.2. Cluster assisted σ-bond activation

With the addition of the third methane ligand, our experimental data indicate σ-bond activation becomes competitive with adduct formation, $Ti(CH_4)_3^+$, $(CH_4)_2Ti(H)(CH_3)^+$, and $(CH_4)Ti(CH_3)_2^+$ are all observed. The $(CH_4)_2Ti(H)(CH_3)^+$ and $Ti(CH_4)_3^+$ clusters are clearly distinguishable in our experiment even though they have the same mass [17]. The observed free energies, ΔG, as a function of temperature for these equilibria [reactions (3a) and (3b)] are shown in Fig. 3

$$Ti^+(CH_4)_2 + CH_4 \rightleftharpoons Ti^+(CH_4)_3 \quad (3a)$$

$$CH_4Ti^+\begin{matrix}H\\ \diagup\\ \diagdown\\ CH_3\end{matrix} + CH_4 \rightleftharpoons (CH_4)_2Ti^+\begin{matrix}H\\ \diagup\\ \diagdown\\ CH_3\end{matrix} \quad (3b)$$

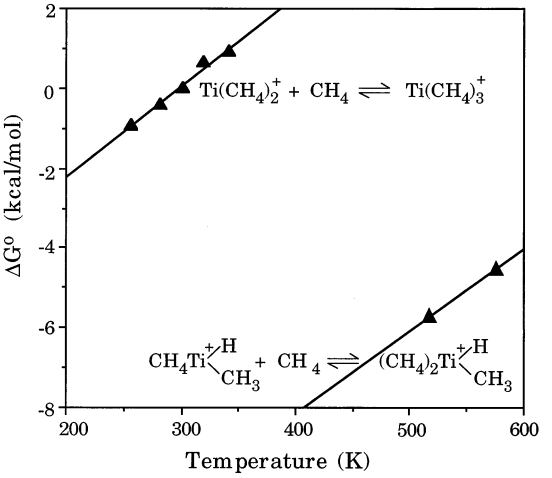

Fig. 3. The plots of ΔG° vs. temperature for the addition of CH_4 to $Ti(CH_4)_2^+$ and $CH_4Ti(H)(CH_3)^+$ ions.

At low temperatures (255–340 K) addition of CH_4 to $Ti(CH_4)_2^+$ comes quickly into equilibrium ($t \ll 500$ μs) indicating simple adduct formation is occurring [reaction (3a)] with ΔH_T° and ΔS_T° values of -6.8 ± 1.3 kcal/mol and -22.7 ± 4.2 cal/mol K, respectively. At high temperatures (500–580 K) addition of CH_4 occurs very slowly and equilibrium is obtained only at very long times ($t > 3000$ μs) indicating σ-bond activation is occurring [reaction (3b)]. A linear fit to the ΔG_T° versus temperature data (Fig. 3) for reaction (3b) gives approximate ΔH_0° and ΔS_T° values of -16 kcal/mol and -21 cal/mol K, respectively (Table 3). Theoretically, reaction (3a) was found to be 2.3 kcal/mol exothermic and reaction (3b), 9.1 kcal/mol exothermic. The relative binding energies agree with those determined by experiment, although the absolute values are underestimated in both cases by several kilocalories per mole.

The rate of the slow approach to equilibrium, associated with C–H bond activation (reaction 4), has a positive energy dependence, as shown in the plot of $-\ln k$ versus $1/T$ (Fig. 4).

$$Ti(CH_4)_2^+ + CH_4 \rightarrow (CH_4)_2Ti^+\begin{matrix}CH\\ \diagup\\ \diagdown\\ CH_3\end{matrix} \quad (4)$$

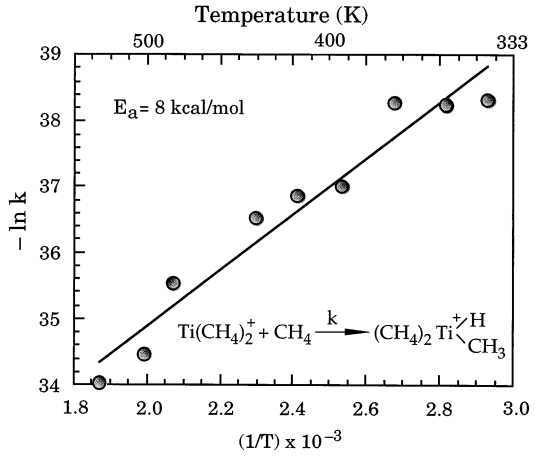

Fig. 4. A plot of $-\ln k$ vs. $1/T$ for the activation of CH_4 by $Ti(CH_4)_2^+$. The activation energy barrier, E_a, to C–H insertion, obtained from the slope of this plot is 8 kcal/mol.

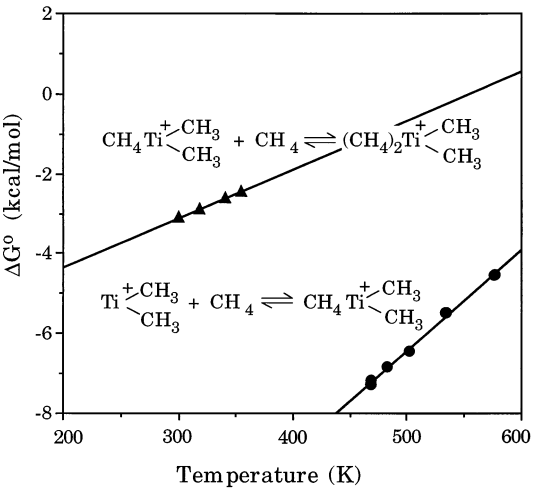

Fig. 5. The plots of $\Delta G°$ vs. temperature for the addition of CH_4 to $Ti(CH_3)_2^+$ and $CH_4Ti(CH_3)_2^+$ ions.

A linear least squares fit to the data yields a barrier to insertion of 8 kcal/mol.

Once H_2 is eliminated, the equilibria for methane loss from, and methane addition to, $(CH_4)Ti(CH_3)_2^+$ are observed [reactions (5a) and (5b)].

$$Ti^+(CH_3)_2 + CH_4 \rightleftharpoons CH_4Ti^+(CH_3)_2 \quad (5a)$$

$$CH_4Ti^+(CH_3)_2 + CH_4 \rightleftharpoons (CH_4)_2Ti^+(CH_3)_2 \quad (5b)$$

The ΔG_T° versus temperature data (Fig. 5) for reaction (5a) yield ΔH_0° and ΔS_T° values of -19.1 ± 0.8 kcal/mol and -25.4 ± 1.5 cal/mol K, respectively (Table 3), in reasonable agreement with the theoretical binding energy of $D_0 = 14.1$ kcal/mol. The 0 K association enthalpy, $\Delta H_0^\circ = -6.8 \pm 0.2$ kcal/mol, for adding a second methane to $Ti(CH_3)_2^+$ [reaction (5b)] is much smaller than the value for adding the first methane [reaction (5a)]. In addition, the association entropy is much larger, $\Delta S_T^\circ = -12.3 \pm 0.7$ cal/mol K, indicating the second methane is farther from the metal center than the first methane and hence more mobile. Replacing one of the methyl groups with a hydrogen atom, $(CH_4)Ti(H)(CH_3)^+$, reduces steric hindrance and results in a stronger binding energy for the remaining CH_4 group, $\Delta H_0^\circ = -16$ kcal/mol, and a more negative association entropy, $\Delta S_T^\circ = -21$ cal/mol K (reaction 2b). The calculated structure for $(CH_4)_2Ti(H)(CH_3)^+$ is also shown in Fig. 6.

To better understand the origin of the observed equilibria, we have calculated important points on the potential energy surfaces for dehydrogenation of clusters of up to three methanes, as shown in Figure 7. The energetics are given in Table 4. A first step in the dehydrogenation of methane must be insertion into a C–H bond to form a $Ti(H)(CH_3)^+$ complex. The formation of Ti–H and Ti–C bonds necessitates a change of spin from quartet to doublet. For a single methane, $Ti(H)(CH_3)^+$ has C_s symmetry with a H–Ti–C angle of 106.5°. The geometries of $Ti(CH_4)^+$ and $Ti(H)(CH_3)^+$ are shown in Fig. 8. The insertion complex is calculated to be uphill with respect to the $Ti(CH_4)^+$ molecular complex by 13.1 kcal/mol at 0 K. Even so, this is still 2.6 kcal/mol below the $Ti^+ + CH_4$ asymptote. However, at 298 K, formation of the insertion complex is calculated to be unfavorable with $\Delta G = +1.6$ kcal/mol. These results are in reasonable agreement with Hendrickx et al. [3] who calcu-

Table 3
Experimental ΔH_0° and ΔS_T° for the reactions indicated

Reaction	Experiment[a,b] $-\Delta H_0^\circ$	Experiment[c] $-\Delta S_T^\circ$	Temperature range[c]	Theory[a] D_0	Theory[c] $-\Delta S$ (298 K)
$Ti^+(CH_3)_2 + CH_4 \rightleftharpoons (CH_4)Ti^+(CH_3)_2$	19.1 ± 0.8	25.4 ± 1.5	470–580	14.1	22.0
$(CH_4)Ti^+(CH_3)_2 + CH_4 \rightleftharpoons (CH_4)_2Ti^+(CH_3)_2$	6.8 ± 0.2	12.3 ± 0.7	300–355	...	...
$(CH_4)Ti^+(CH_3)(H) + CH_4 \rightleftharpoons (CH_4)_2Ti^+(CH_3)(H)$	~16[d]	~21	500–580	9.2	28.8

[a] In units of kcal mol^{-1}.
[b] The uncertainties reflect the uncertainties in ΔH_T° in addition to the uncertainties due to the statistical mechanical modeling.
[c] ΔS_T° values are in units of cal mol^{-1} K^{-1} for the temperature range, T, in units of K.
[d] This value is approximate because equilibrium was obtained at only two temperatures.

lated $Ti(H)(CH_3)^+$ to be 1.1 kcal/mol above the $Ti^+ + CH_4$ asymptote at 0 K, only 3.7 kcal/mol higher in energy than our results. Hendrickx et al. [3] also calculated the transition state for insertion to lie 15.3 kcal/mol above the $Ti^+ + CH_4$ asymptote. Thus, insertion into a C–H bond of $Ti(CH_4)^+$ to form $Ti(H)(CH_3)^+$ is not expected to occur under the conditions of our experiment.

With a second methane coordinated to the metal, insertion into a single C–H bond is still energetically unfavorable with respect to the molecular complex, but overall more exothermic with respect to the separated fragments. Insertion into a C–H bond of $Ti(CH_4)_2^+$ to yield $Ti(H)(CH_3)(CH_4)^+$ is calculated to be uphill by 13.4 kcal/mol, comparable to the relative energetics of $Ti(CH_4)^+$ and $Ti(H)(CH_3)^+$. On the other hand, the insertion complex is calculated to be below the $Ti^+ + 2CH_4$ asymptote by 17.1 kcal/mol at 0 K. At 298 K, however, C–H bond activation becomes favorable with $\Delta G = -3.6$ kcal/mol. Even so, direct formation of the insertion complex is probably prevented by a barrier which lies above the zero of energy. This barrier is expected to be comparable in relative height to that for activation of the first methane.

Insertion into a C–H bond of $Ti(CH_4)_3^+$ to yield $Ti(H)(CH_3)(CH_4)_2^+$ is substantially easier, being uphill by only 6.1 kcal/mol. Overall, formation of this inserted complex is exothermic by 26.3 kcal/mol at 0

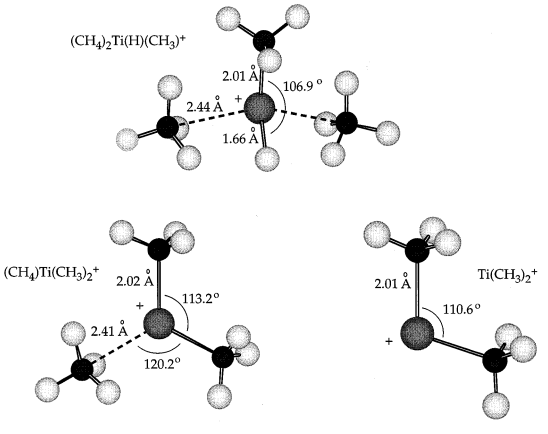

Fig. 6. Geometries of the $(CH_4)_2Ti(H)(CH_3)^+$, $(CH_4)Ti(CH_3)_2^+$, and $Ti(CH_3)_2^+$ complexes calculated.

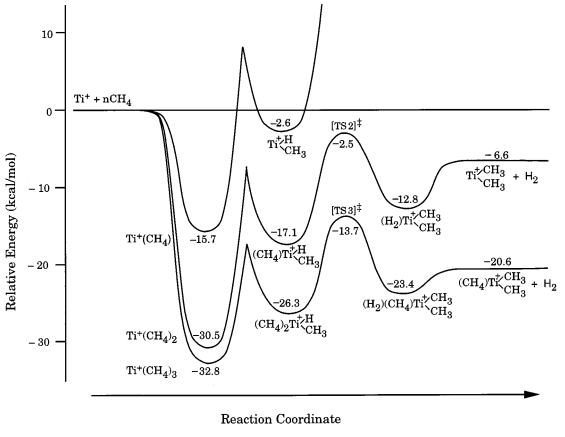

Fig. 7. Theoretical potential energy surfaces at 0 K for the dehydrogenation of methane. The initial molecular clusters are quartet and a spin change to doublet occurs upon methane activation as shown by the sharply pointed transition states. The barriers associated with this first C–H bond activation have not been calculated and are shown here only schematically. Enthalpies (in kcal/mol) including zero-point energy corrections relative to the $Ti^+ + nCH_4$ asymptotes are given explicitly.

Table 4
Energetic data for all species relative to the $Ti^+ + nCH_4$ asymptotes

	ΔH (0 K)[a]	ΔH (298 K)[a]	ΔS (298 K)[b]	ΔG (298 K)[a]
$Ti(CH_4)^+$	−15.7	−15.4	−17.3	−10.3
$Ti(H)(CH_3)^+$	−2.6	−3.1	−15.5	+1.6
Transition state [TS 1]‡	+17.7	+18.0	−17.2	+23.2
$Ti(CH_2)(H_2)^+$	+18.0	+18.1	−17.0	+23.1
$Ti(CH_2)^+ + H_2$	+29.3	+30.5	+11.1	+27.2
$Ti(CH_4)_2^+$	−30.5	−30.0	−45.3	−16.5
$Ti(H)(CH_3)(CH_4)^+$	−17.1	−16.9	−44.5	−3.6
Transition state [TS 2]‡	−2.5	−2.3	−47.3	+11.9
$Ti(CH_3)_2(H_2)^+$	−12.8	−12.1	−42.5	+0.5
$Ti(CH_3)_2^+ + H_2$	−6.6	−4.8	−18.4	+0.7
$Ti(CH_2)(CH_4)^+ + H_2$	+14.4	+16.3	−18.3	+21.8
$Ti(CH_4)_3^+$	−32.8	−31.5	−63.4	−12.6
$Ti(H)(CH_3)(CH_4)_2^+$	−26.3	−25.8	−73.3	−4.0
Transition state [TS 3]‡	−13.7	−13.1	−74.2	+9.0
$Ti(CH_3)_2(H_2)(CH_4)^+$	−23.4	−22.2	−69.1	−1.6
$Ti(CH_3)_2(CH_4)^+ + H_2$	−20.6	−18.6	−40.4	−6.5
$Ti(CH_2)(CH_4)_2^+ + H_2$	+0.8	+3.0	−50.0	+17.9

[a] In units of kcal mol^{-1}.
[b] In units of cal mol^{-1} K^{-1}.

K with respect to the $Ti^+ + 3CH_4$ asymptote and spontaneous at 298 K, $\Delta G = -4.0$ kcal/mol. The barrier for activation of the third methane is expected to be smaller than that for activation of either the first or second methane due to the more favorable relative energetics for formation of the insertion complex. Should all initial internal energy be preserved upon collision with the third methane (i.e. intermediate $Ti(CH_4)_n^+$ clusters have not been stabilized through collisions) then the insertion complex is likely directly formed under the experimental conditions. Indeed, formation of the $Ti(H)(CH_3)(CH_4)_2^+$ complex opens up a channel to form $Ti(H)(CH_3)(CH_4)^+$ through a loss of a methane ligand resulting in the equilibrium observed [reaction (3b)]. The methane complexation energy for this reaction is calculated to be exothermic by 9.1 kcal/mol in reasonable agreement with the approximate experimental BDE of 16 kcal/mol.

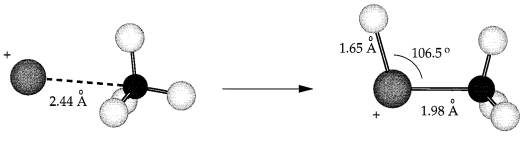

Fig. 8. Calculated geometries of $Ti(CH_4)^+$ and $Ti(H)(CH_3)^+$.

Activation of a second C–H bond in these complexes to lead to H–H bond formation is the next step in the dehydrogenation process. While $Ti(H)(CH_3)^+$ is not expected to be formed, it is useful to consider the loss of H_2 from this species to form a metal methylidene. Dehydrogenation may be expected to proceed through insertion into a second C–H bond of the methyl group to form $Ti(CH_2)(H_2)^+$ followed by loss of H_2 to form doublet $TiCH_2^+$. However, the reaction $Ti^+ + CH_4 \rightarrow TiCH_2^+ + H_2$ was calculated to be endothermic by 29.29 kcal/mol and not spontaneous, $\Delta G = +27.2$ kcal/mol, at 298 K. Experimentally, this reaction has been determined by Sunderlin and Armentrout to be endothermic by 18.9 kcal/mol [15]. Both theory and experiment agree in this case that dehydrogenation of a single methane should not be observed under the present conditions. To complete the potential energy surface for the reaction, the energetics of the $Ti(CH_2)(H_2)^+$ complex and $Ti(CH_2)(H_2)^+ \rightleftharpoons Ti(H)(CH_3)^+$ transition state were calculated. The intermediate $Ti(CH_2)(H_2)^+$ complex is unstable by 18.1 kcal/mol. In fact, the complex collapses to the $Ti(H)(CH_3)^+$ intermediate with virtually no barrier (the transition state was calculated to be unstable by 18.0 kcal/mol).

For addition of the second and third methane, dehydrogenation could potentially proceed through a similar pathway, but this appears to be energetically unfavorable. The reaction $Ti^+ + 2CH_4 \rightarrow Ti(CH_2)(CH_4)^+ + H_2$ was calculated to be endothermic by 16.3 kcal/mol. The reaction $Ti^+ + 3CH_4 \rightarrow Ti(CH_2)(CH_4)_2^+ + H_2$ was calculated to be endothermic by only 3.0 kcal/mol, but is strongly entropically disfavored with $\Delta G = +17.9$ kcal/mol at 298 K. Considering possible underestimation of the theoretical binding energies as compared with experiment (~10 kcal/mol for the Ti = CH_2 bond and ~2–5 kcal/mol for each Ti–CH_4 bond), dehydrogenation of the third methane to form $Ti(CH_2)(CH_4)_2^+$ may actually be energetically favorable and cannot be completely ruled out by the calculations. Yet another pathway for dehydrogenation appears more likely for complexes containing two and three methanes.

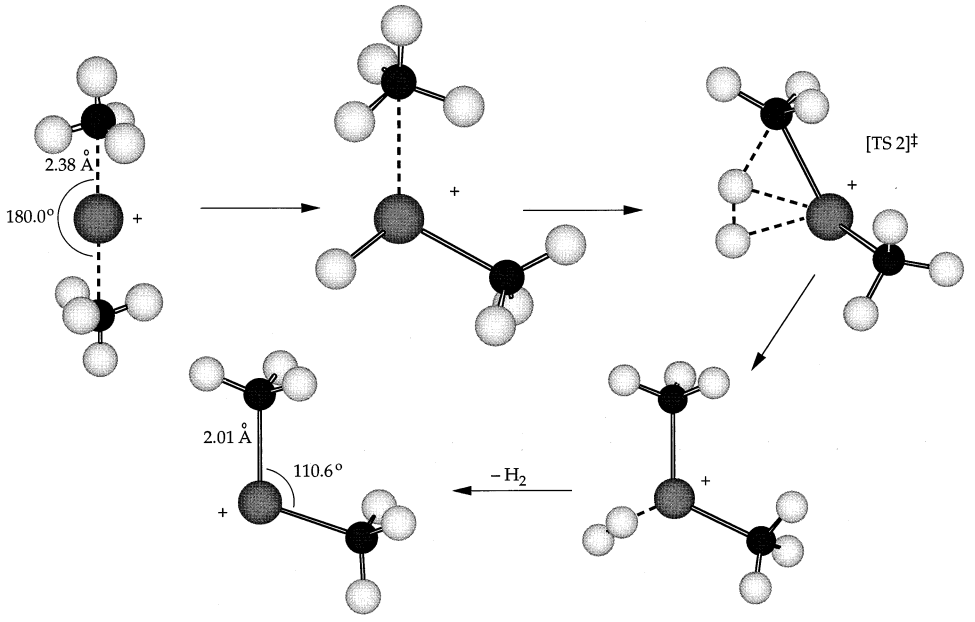

Fig. 9. Calculated geometries of $Ti(CH_4)_2^+$, $Ti(H)(CH_3)(CH_4)^+$, transition state 2, $[TS\ 2]^‡$, $Ti(CH_3)_2(H_2)^+$, and $Ti(CH_3)_2^+$.

After activation of one methane in the clusters $Ti(CH_4)_2^+$ and $Ti(CH_4)_3^+$ to form the intermediate complexes $Ti(H)(CH_3)(CH_4)^+$ and $Ti(H)(CH_3)(CH_4)_2^+$, it is possible to insert into a second C–H bond from a second methane to form the dimethyl complexes $Ti(CH_3)_2(H_2)^+$ and $Ti(CH_3)_2(H_2)(CH_4)^+$, reactions (6) and (7). The calculated heats and free energies of reaction are indicated

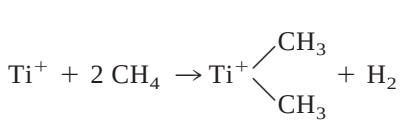

	ΔH_0 (kcal/mol)	ΔG_{298} (kcal/mol)	
$Ti^+ + 2\,CH_4 \rightarrow Ti^+(CH_3)_2 + H_2$	−6.6	+0.70	(6)
$Ti^+ + 3\,CH_4 \rightarrow (CH_4)Ti^+(CH_3)_2 + H_2$	−18.6	−6.5	(7)

Both reactions are considerably more favorable than dehydrogenation via formation of a metal methylidene bond, and considering errors in the calculated binding energies, both reactions are expected to be exothermic at room temperature. These calculations suggest that dehydrogenation occurs via formation of a dimethyl structure. The geometries for the participants in reactions (6) and (7) are shown in Figs. 9 and 10, respectively. Experimentally we observe C–H bond activation only after the addition of the third methane probably due to the rapid thermalization of the $Ti(CH_4)_2^+$ adduct. Once dehydrogenation occurs, the equilibrium for the elimination/addition of a single methane to this species is observed. For the dimethyl

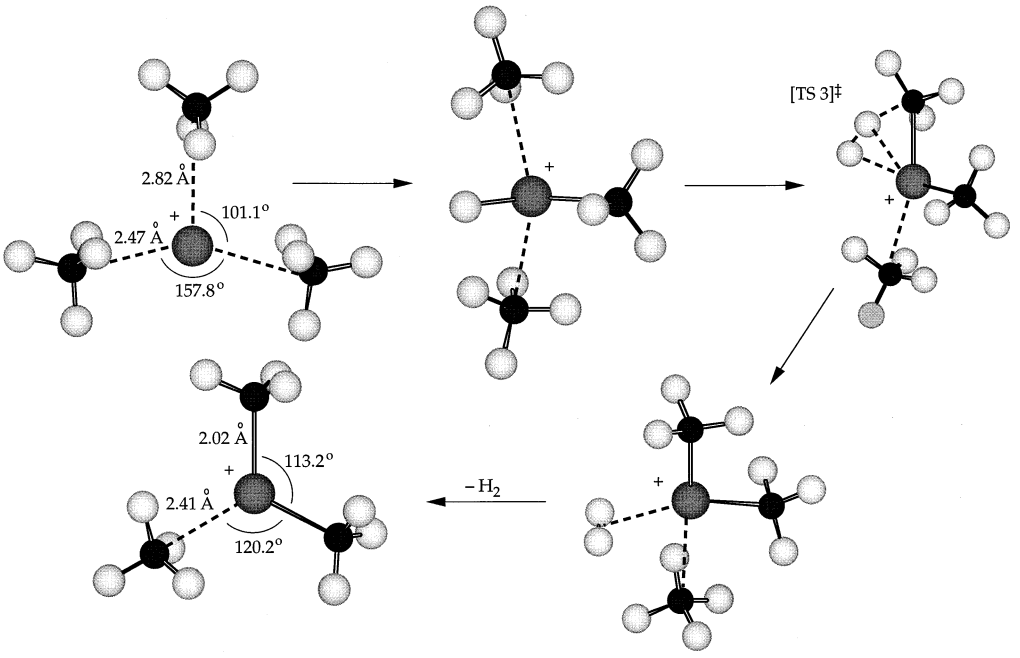

Fig. 10. Calculated geometries of $Ti(CH_4)_3^+$, $Ti(H)(CH_3)(CH_4)_2^+$, transition state 3, $[TS\ 3]^‡$, $Ti(CH_3)_2(H_2)(CH_4)^+$, and $Ti(CH_3)_2(CH_4)^+$.

product ion, $(CH_4)Ti(CH_3)_2^+$, a single methane loss to produce $Ti(CH_3)_2^+$ is reasonable. If the dehydrogenation produced the methylydene structure, $(CH_4)_2TiCH_2^+$, we would expect to see the loss of two successive methanes, inconsistent with the experimental results. Thus, both theoretical and experimental results indicate that dehydrogenation occurs via formation of a dimethyl structure.

The important aspects of the potential energy surfaces for the dehydrogenation of $Ti(CH_4)_2^+$ and $Ti(CH_4)_3^+$ were completed by characterizing the $Ti(CH_3)_2(H_2)^+$ and $Ti(CH_3)_2(H_2)(CH_4)^+$ intermediates and the $Ti(H)(CH_3)(CH_4)^+ \rightleftharpoons Ti(CH_3)_2(H_2)^+$ and $Ti(H)(CH_3)(CH_4)_2^+ \rightleftharpoons Ti(CH_3)_2(H_2)(CH_4)^+$ transition states ($[TS\ 2]^‡$ and $[TS\ 3]^‡$) with the structures given in Figs. 9 and 10, respectively. The $Ti(CH_3)_2(H_2)^+$ complex was found to be stable by 12.8 kcal/mol at 0 K and the $Ti(CH_3)_2(H_2)(CH_4)^+$ complex was found to be stable by 23.4 kcal/mol at 0 K. The latter result suggests that $Ti(CH_3)_2(H_2)(CH_4)^+$ is not stable with respect to loss of H_2 at room temperature, as a significant amount of entropy is released upon dehydrogenation. As for the transition states for formation of these intermediates, the barrier for $Ti(CH_3)_2(H_2)^+$ lies 2.5 kcal/mol below the $Ti^+ + 2CH_4$ asymptote at 0 K and the barrier for $Ti(CH_3)_2(H_2)(CH_4)^+$ lies 13.7 kcal/mol below the $Ti^+ + 3CH_4$ asymptote at 0 K. Both of these barriers are probably lower than calculated due to underestimation of the binding energies.

The schematic potential energy surfaces for the sequential addition of three CH_4 molecules and the subsequent loss of H_2 based on experimentally determined energies is shown in Fig. 11. One important difference between the potential energy surfaces based on theory (Fig. 7) and those based on experiment (Fig. 11) are the energies of the $Ti(H)(CH_3)^+$, $(CH_4)Ti(H)(CH_3)^+$ and $(CH_4)_2Ti(H)(CH_3)^+$ complexes relative to their respective association complexes, $Ti(CH_4)_n^+$, $n = 1, 2, 3$. Even though the $Ti(H)(CH_3)^+$ complex is calculated to be 2.6 kcal/mol below the $Ti^+ + CH_4$ asymptote (Fig. 7) it is estimated to be 10 kcal/mol lower in energy experimentally (Fig. 11). Analogously, the experimental $(CH_4)Ti(H)(CH_3)^+$ and $(CH_4)_2Ti(H)(CH_3)^+$ complexes are also lower in energy. Both theory and

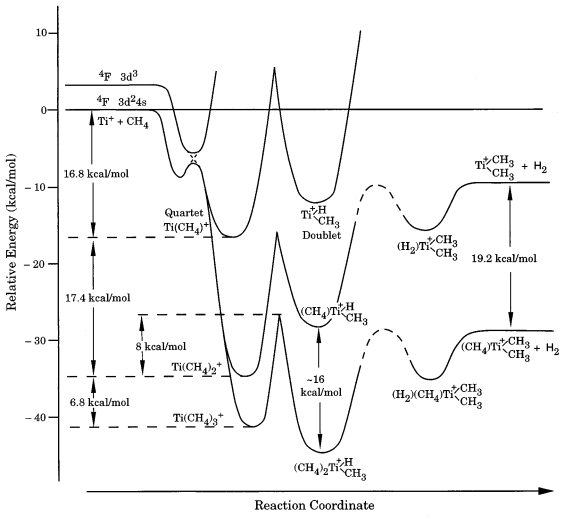

Fig. 11. Schematic potential energy surface for the sequential addition of three CH_4 molecules to ground state $Ti^+(^4F)$ and the subsequent loss of H_2 to produce $CH_4Ti(CH_3)_2^+$. The successive binding energies for the $Ti(CH_4)_n^+$ clusters measured are indicated. These clusters are bound on the quartet surface and C–H bond activation requires a spin change to the doublet surface as shown by the sharply pointed transition states. All other transition states are adiabatic. The C–H bond activation energy barrier is measured to be 8 kcal/mol. The location at which the spin change from the quartet to the doublet occurs and the transition state for C–H bond activation are not necessarily the same, but are shown to be the same for simplicity only. The location of the $Ti(CH_3)_2^+ + H_2$ asymptote was estimated from binding energies of Ti^+–CH_3 and CH_3Ti^+–CH_3 measured by Sunderlin and Armentrout [15,16]. The dashed portion of the surface indicates greater uncertainty in the energetics.

experiment indicate formation of the inserted intermediate, $(CH_4)Ti(H)(CH_3)^+$, to be energetically less favorable than the association complex, $Ti(CH_4)_2^+$, and therefore, simple adduct formation will dominate for Ti^+ reacting with two methanes. However, in contrast to theory, experiments indicate $(CH_4)_2Ti(H)(CH_3)^+$ is energetically favored over $Ti(CH_4)_3^+$, making σ-bond activation competitive with simple adduct formation.

From both the theoretical and experimental data, we can extract the cluster assisted σ-bond activation mechanism for dehydrogenation of methane as shown in Scheme 1.

Conclusion

We have determined sequential binding energies and entropies for the clustering of Ti^+ with methane, $Ti(CH_4)_n^+$, $n = 1$–5, via temperature-dependent equilibrium measurements. The BDEs for $n = 1$–5 are 16.8, 17.4, 6.6, 9.8, and 5.1 kcal/mol, respectively, in good agreement with theory. A first solvation sphere of four methanes is observed. The fifth methane is farther away from the metal center in a new solvation sphere where it is less tightly bound and has greater translational freedom, reflected in a much larger association entropy. Theoretical results indicate that the nonmonotonic variation in BDEs is due to the fact that s–d hybridization is beneficial for the first two methane ligands only and significant changes to the electronic structure are required with the addition of the third and fourth methane ligands.

For the addition of the third methane ligand to Ti^+, we observed σ-bond activation to be competitive with adduct formation. The $Ti(CH_4)_3^+$ adduct produced in a fast equilibrium at low temperatures (255–340 K) is

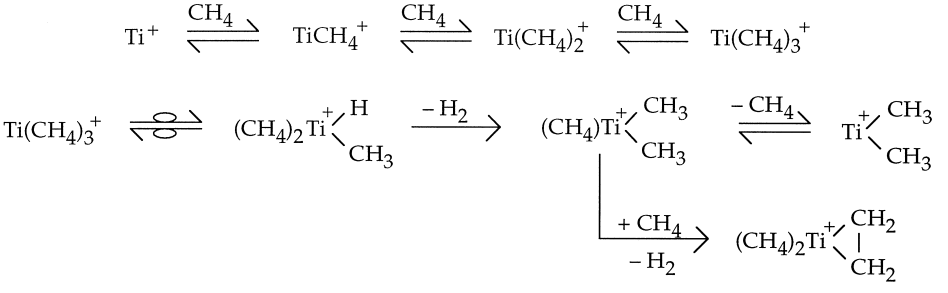

Scheme 1.

clearly distinguishable from the $(CH_4)_2Ti(H)(CH_3)^+$ cluster produced with a positive temperature dependence at higher temperatures (340–550 K). A barrier to insertion of 8 kcal/mol was determined. Dehydrogenation of the $(CH_4)_2Ti(H)(CH_3)^+$ cluster produced $(CH_4)Ti(CH_3)_2^+$ and the addition of a fourth methane resulted in further dehydrogenation and formation of an ethylene ligand bound to the metal center, $(CH_4)_2Ti(C_2H_4)^+$.

The trend in BDEs observed for $Ti(CH_4)_n^+$, $n = 1–4$, parallels that observed for $Co(CH_4)_n^+$. However, the BDEs for $Co(CH_4)_n^+$ are larger (by ~6 kcal/mol) than the corresponding $Ti(CH_4)_n^+$ values, due to the smaller size of Co relative to Ti. In contrast with the Ti^+/CH_4 system, σ-bond activation is not observed for Co^+ reacting with methane. For late first-row transition-metal ions, including cobalt, formation of inserted intermediates, $(CH_4)_nM(H)(CH_3)^+$, cannot compete effectively with adduct formation, $M(CH_4)_n^+$, because they are relatively less stable.

The clustering of methane ligands to Ti^+ clearly shows the effects of progressive ligation and ultimately provides a detailed understanding of σ-bond activation processes.

Acknowledgements

We gratefully acknowledge the support of the National Science Foundation under grant no. CHE-9729146. We also thank Professor P. Maître for helpful discussion.

References

[1] P.B. Armentrout, in D.H. Russel (Ed.), Gas Phase Inorganic Chemistry, Plenum, New York, 1989.
[2] C.W. Bauschlicher, H. Partridge, J.A. Sheehy, S.R. Langhoff, M.J. Rosi, Chem. Phys. 96 (1992) 6969.
[3] M. Hendrickx, M. Ceulemans, K. Gong, L. Vanquickenborne, J. Phys. Chem. A 101 (1997) 2465. In this study, CASSCF calculations were used to obtain structures and CASPTZ calculations on the CASSCF structures were done to incorporate the dynamical correlation effects in the energy calculations.
[4] R. Tonkyn, M. Ronan, J.C. Weisshaar, J. Phys. Chem. 92 (1988) 92.
[5] P.R. Kemper, J.E. Bushnell, P.A.M. van Koppen, M.T. Bowers, J. Phys. Chem. 97 (1993) 1810.
[6] C.L. Haynes, P.B. Armentrout, J.K. Perry, W.A. Goddard III, J. Phys. Chem. 99 (1995) 6340.
[7] R.H. Schultz, P.B. Armentrout, J. Phys. Chem. 97 (1993) 596.
[8] Y.A. Ranasinghe, T.J. MacMahon, B.S. Freiser, J. Phys. Chem. 95 (1992) 7721. Contribution of electronically excited Zr^+ to the data was not resolved.
[9] P.A.M. van Koppen, P.R. Kemper, J.E. Bushnell, M.T. Bowers, J. Am. Chem. Soc. 117 (1995) 2098.
[10] K.K. Irikura, J.L. Beauchamp, J. Phys. Chem. 95 (1991) 8344.
[11] R. Wesendrup, D. Schroder, H. Schwarz, Angew. Chem. Int. Engl. 33 (1994) 1174.
[12] J.E. Bushnell, P.R. Kemper, P. Maître, M.T. Bowers, J. Am. Chem. Soc. 116 (1994) 9710.
[13] A.K. Rappe, T.H. Upton, J. Chem. Phys. 85 (1986) 4400.
[14] The HTi^+CH_3, bond energy is estimated from measured $Ti^+–H$, $Ti^+–CH_3$, and $CH_3Ti^+–CH_3$ bond energies [15,16].
[15] L.S. Sunderlin, P.B. Armentrout, J. Phys. Chem. 92 (1988) 1209.
[16] L.S. Sunderlin, P.B. Armentrout, Int. J. Mass Spectrom. Ion Processes 94 (1989) 149.
[17] P.R. Kemper, M.T. Bowers, J. Am. Soc. Mass Spectrom. 1 (1990) 197.
[18] P.R. Kemper, M.T. Bowers, J. Phys. Chem. 95 (1991) 5134.
[19] Surface ionization of $TiCl_4$ produces 36% $Ti^+(^4F, 3d^3)$, the first excited state. Ion chromatography experiments [18] indicate this state is effectively quenched to ground state Ti^+ $(^4F, 4s3d^2)$ in collisions with CH_4.
[20] P.R. Kemper, J.E. Bushnell, P.A.M. van Koppen, M.T. Bowers, J. Phys. Chem. 97 (1993) 1810.
[21] A.D. Becke, Phys. Rev. A 38 (1988) 3098; C. Lee, W. Yang, R.G. Parr, Phys. Rev. B 37 (1988) 785; implemented as described in B. Miehlich, A. Savin, H. Stoll, H. Preuss, Chem. Phys. Lett. 157 (1989) 200.
[22] P.J. Hay, W.R. Wadt, J. Chem. Phys. 82 (1985) 299.
[23] W.J. Hehre, J.A. Pople, J. Chem. Phys. 56 (1972) 4233.
[24] R. Krishnan, J.S. Binkley, R. Seeger, J.A. Pople, J. Chem. Phys. 72 (1980) 650; M.J. Frisch, J.A. Pople, and J.S. Binkley, ibid. 80 (1984) 3265.
[25] JAGUAR 3.5, Schrödinger, Inc., Portland, OR, 1998.
[26] J.K. Perry, G. Ohanessian, W.A. Goddard III, J. Phys. Chem. 97 (1993) 5238.
[27] P.R. Kemper, P. Weis, P. Maître, M.T. Bowers, J. Am. Chem. Soc. 120 (1998) 13494.
[28] P.R. Kemper, P. Weis, M.T. Bowers, Chem. Phys. Lett. 293 (1998) 503.
[29] P.A.M. van Koppen, P. Weis, J.K. Perry, P.R. Kemper, unpublished.